https://doi.org/10.48048/tis.2025.9391

Biosynthesis of Selenium Nanoparticles and Selenium-Enriched γ-Polyglutamic Acid (Se-PGA) by *Bacillus subtilis*

Suthima Likidtaveesin[1], Napawan Changtong[1], Nongpanga Jarussophon[2] and Orawan Chunhachart[1,*]

[1]Division of Microbiology, Department of Science and Bioinnovation, Faculty of Liberal Arts and Science, Kasetsart University, Kamphaeng Saen Campus, Nakhon Pathom 73140, Thailand
[2]Division of Chemistry, Department of Physical and Material Sciences, Faculty of Liberal Arts and Science, Kasetsart University, Kamphaeng Saen Campus, Nakhon Pathom 73140 Thailand

([*]Corresponding author's e-mail: orawan.chu@ku.th)

Received: 26 November 2024, Revised: 25 December 2024, Accepted: 1 January 2025, Published: 20 February 2025

Abstract

Biogenic synthesized selenium nanoparticles (SeNPs) have garnered significant interest in both biomedical and agricultural fields. Encapsulation of SeNPs by natural biopolymers can increase the stability and biocompatibility of the nanoparticles. In this work, synthesis of SeNPs by *Bacillus subtilis* NT147, γ-polyglutamic acid (γ-PGA) producing strain and production of Se-enriched γ-PGA (Se-PGA) were carried out. *B. subtilis* NT147 was cultured in Luria Bertani broth supplemented with 0.5 mM Na_2SeO_3 at 37 ± 2 °C with shaking at 150 rpm. From ICP analysis, the selenium amount in the bacterial cells was highest at 18 h (11.3 mg/g cell DW). The TEM image confirmed that SeNPs were spherical shape and produced mainly in the bacterial cells. Particle size analysis using a laser scattering particle size distribution analyzer indicated that small particle sizes 226 and 259 nm were observed at 6 and 12 h, respectively. Poor dispersion and aggregation of SeNPs were observed after 12 h, resulting in larger particles. Production of γ-PGA significantly decreased when Na_2SeO_3 was presented in the culture media. Therefore, *B. subtilis* NT147 was cultured in a sucrose yeast extract medium containing 5 % sucrose at 37 ± 2 °C with shaking at 150 rpm for 36 h to maximized γ-PGA yield. Then 2.5 mM Na_2SeO_3 was added into the culture medium and continued shaking for 4 h. Cells were removed and Se-PGA was precipitated. SEM image showed a spherical shape of SeNPs dispersed in γ-PGA and the EDS confirmed the presence of Se, C, N and O in the Se-PGA composite suggesting that SeNPs were mainly came out after cell lysis. FTIR spectra of Se-PGA showed peak, indicating the presence of carbonyl and hydroxyl groups, suggesting proteins and amino acids. The Se-PGA at a concentration of 2.0 g/L exhibited 17.96 % of inhibition against *Colletotrichum* sp.

Keywords: Selenium nanoparticles, Bioactive nanoparticles, Green synthesis, γ-Polyglutamic acid, Antifungal activity

Introduction

Selenium is an element that is essential for living things and has lower toxicity than selenite, selenate and selenide. Se-containing foods have become more popular in the functional food market in recent years. Traditional Se-containing supplements are mainly inorganic Na_2SeO_3 and organic Se ingredients, such as SeMet, SeCys and selenized yeast [1]. The toxicity of inorganic selenium is more than 40 times that of the organic form based on the basis of LD_{50} determination [2,3]. Although organic Se supplementation has many advantages, such as low toxicity and high bioavailability, the presently marked organic selenized yeast or Se-amino acid chelate has quality issues, including instability and mixing with inorganic Se. In addition to the advantages of traditional organic Se, organic SeNPs have specific biological activity [4]. Selenium nanoparticles (SeNPs) have garnered significant interest in recent years due to their unique

properties and potential applications in various fields, including medicine [5], foods, agriculture [6] and environments [7]. The physical and chemical synthesis of SeNPs have disadvantages such as high production costs, being environmentally unfriendly, high energy consumption and biocompatibility problems [4,8]. Currently, researchers are increasingly interested in synthesizing selenium nanoparticles through biological methods using plant extracts and microorganisms [1]. Oraganic SeNPs obtained by green synthesis methods can have enhanced bioactivity, this approach reduces the use of toxic chemicals and is more environmentally friendly. Furthermore, the biomolecules present in microorganisms and plant extracts can act as both reducing agents and stabilizers, resulting in lower production costs [9,10]. The biological properties of SeNPs depend on their particle size, and encapsulating SeNPs can help improve their stability properties [11,12]. Chemical green synthesis of SeNPs can be achieved in various ways, such as reducing selenite with ascorbic acid along with the addition of polysaccharides like chitosan [9], glucomannan [13] and carboxymethyl cellulose [14] to stabilize the nanoparticles. Additionally, it was found that synthesizing selenium nanoparticles using ascorbic acid along with chitosan and γ-polyglutamic acid (γ-PGA) to enhance stability resulted in CS-SeNPs and PGA-SeNPs with particle sizes of approximately 100 nm which are smaller than SeNPs synthesized without chitosan and γ-PGA [15]. These biopolymers result in the biocompatibility of the composite and selenium nanoparticles, making the selenium nanoparticles stable, non-toxic and biodegradable, these composites are suitable for consumption and can be applied in medical, nutritional and agriculture [4].

Synthesizing SeNPs using microorganisms offers advantages over plant extract synthesis methods because the nanoparticles produced through this method are highly pure, spherical and uniform, with their size depending on the type of microorganism used [8,16]. The reduction of selenite by bacteria can occur under both aerobic and anaerobic conditions [2,17]. This biotransformation leads to the formation of cytoplasmic, periplasmic or extracellular SeNPs. The mechanism begins with metal ions binding to the surface or within the cell. Subsequently, the metal ions are reduced to nanoparticles under conditions facilitated by enzymes [18]. However, it is also hypothesized that compounds synthesized by microbial cells, such as vitamins, organic acids, polysaccharides, proteins and carbohydrates, play a role in the reduction and act as stabilizing agents [11,19,20]. There are 2 possible mechanisms for biosynthesis: Enzymatic reduction, which uses enzymes as reducing agents [18] and non-enzymatic reduction [21]. Microbial exopolysaccharides (EPS) contain various functional groups including carboxyl, amine, and hydroxyl groups play a critical role by interacting with metal ions during nanoparticle synthesis [22]. *Bacillus* sp. has been shown to produce SeNPs [23-25]. The process of selenite synthesis in *Bacillus* sp. SL involves several reduction pathways, including sulfur assimilation, glutathione reduction, periplasmic reduction enzymes and the sulfuroxygen reduction system. Extracellular selenite enters the bacterial cell via the sulfate adenylyltransferase process, where it is reduced through pathways like sulfur assimilation, glutathione reduction and periplasmic enzymes. Electrons from outside the cell help reduce selenite to elemental selenium [18]. SeNPs produced from *Bacillus megaterium* cell free supernatant has been reported [26]. *Bacillus subtilis* and its related species are recognized to be effective producers of γ-PGA [27,28]. γ-PGA is an edible anionic biopolymer composed of L- and D-glutamate linked by γ-glutamyl bond. It has unique properties such as biodegradability, water solubility, non-toxicity and biocompatibility [29]. γ-PGA has been used for food [30], medical [31] and agricultural fields [32]. A study investigating the effects of γ-PGA on gene expression in *Arabidopsis thaliana* revealed that γ-PGA enhances the expression of genes associated with nitrogen metabolism, a vital component for plant growth, as well as those involved in the phenylpropanoid pathway [33]. Furthermore, γ-PGA influences on the production of indole-3-acetic acid (IAA) and lateral root development in maize. Analysis of genes expression revealed that γ-PGA triggers genes associated with the synthesis of IAA-related enzymes [34].

The availability of selenium to plants plays a crucial role in their physiological condition, allowing for the potential regulation of mineral nutrition to influence specific metabolic aspects [35]. This regulation may

enhance the plants' ability to withstand adverse environmental conditions. Several researches have documented the involvement of selenium in various physiological processes. Seed priming utilizing a mix of SeNPs and zinc nanoparticles (ZnNPs) is an effective strategy for risk mitigation in direct-seeded rice (*Oryza sativa* L.), enhancing germination, growth and yield [36]. The application of Se(IV) resulted in elevated levels of auxin, jasmonic acid and salicylic acid in the leaves, while promoting an increase in cytokinin concentrations in the roots. These modifications in phytohormonal signaling pathways contribute to improved plant growth and heightened resistance to stress. Furthermore, Se(IV) modulates the expression of genes associated with flavonoid biosynthesis, thereby influencing the growth and developmental processes in tomato plants. [37]. Their findings underscore the importance of continued research into the function of selenium in plant physiology. Furthermore, biogenic SeNPs inhibit the growth of the wood brown-rotting fungi [7]. SeNPs coated with γ-PGA enhanced seed germination of sunflower sprouts [15]. Given the properties of selenium nanoparticles and the benefits of γ-PGA, combining these 2 compounds could be potentially beneficial and have significant applications as dietary supplements, agricultural applications or in medical fields. Consequently, the synergistic production of selenium-enriched γ-PGA (Se-PGA) through bacterial fermentation represents a cost-effective approach with potential agricultural applications, including use as fertilizers, plant disease management, and seed coating materials. The trend of producing SeNPs using these bio-factories indicates potential for scaling up production to larger levels and γ-PGA is recognized for its numerous benefits and versatile applications across various fields. However, there is a notable lack of research concerning the synthesis of γ-PGA derivatives with selenium using bacteria. This gap presents an opportunity for exploration into the potential interactions and synergistic effects of these compounds, which could have significant implications in food, biotechnology, agriculture and health sciences. Microbial fermentation could provide feasible and economic approach for production of organic selenium compounds. However, there is still a need for data in terms of microbiology and suitable culture conditions for Se-bearing γ-PGA, which are currently limited especially by the use of selenium-enriched technique. There is also a lack of information concerning the structure and functionality relationship of Se-bering γ-PGA. Therefore, this research aimed to synthesize SeNPs and Se-enriched γ-PGA (Se-PGA) by using *B. subtilis* NT147, a γ-PGA producing strain. The physicochemical properties of SeNPs and Se-PGA were investigated, and antifungal activity of Se-PGA was examined.

Materials and methods

Strain and chemicals

Bacillus subtilis NT147, γ-polyglutamic acid producing strain, was isolated from Thai fermented soybean. The strain was cultured in Luria-Bertani medium (LB) and incubated at 37 ± 2 °C. Sodium selenite (Na_2SeO_3) was purchased from Sigma-Aldrich, USA.

Effect of sodium selenite on the growth of *B. subtilis* NT147

B. subtilis NT147 was cultured on LB agar supplemented with 0 to 50 mM of sodium selenite and incubated at 37 ± 2 °C for 24 h. The growth, colony color and colony morphology were observed. For liquid medium, 18-hour grown *B. subtilis* NT147 was transferred to LB broth, and then the culture was incubated at 37 ± 2 °C with shaking at 150 rpm until the OD_{600} was at 0.5. The cell suspension was transferred into 50 mL of LB broth (1 % inoculum) supplemented with sodium selenite at a final concentration of 0, 0.5, 1.0, 1.5, 2.0 and 2.5 mM, and the cultures were incubated at 37 ± 2 °C for 24 h with shaking at 150 rpm. The samples were withdrawn every 3 h to measure the growth by the dilution plate count method. The medium without sodium selenite supplementation served as a control.

Reduction of selenite in liquid medium

B. subtilis NT147 was grown in LB broth and incubated at 37 ± 2 °C with shaking at 150 rpm until the OD_{600} was at 0.5. The cell suspension (2 % inoculum) was transferred to LB broth containing 0.5 mM sodium selenite and incubated at 37 ± 2 °C with shaking at 150 rpm. The samples were withdrawn at 0, 6, 12, 18, 24 and

36 h. Then cells were removed by centrifugation at 10,000 rpm for 15 min. The supernatant was freeze-dried and cells were washed 3 times with 1.5 M Tris-HCl (pH 8.3) containing 1 % sodium dodecyl sulfate. After that 5 mL of deionized water was added to the cell pellet. Cells were disrupted by using a Bead router (BR Elite, Omni International Co. Ltd., USA) for 10 min. Cell debris was then precipitated with cold ethanol at a ratio of 1:4. The mixtures were left in a refrigerator overnight, then the liquid portion was transferred to a new centrifuge tube and centrifuged at 10,000 rpm for 10 min. The supernatant was discarded and the precipitate was freeze-dried. The freeze-dried culture broth and disrupted cells were analyzed for selenium amount.

Synthesis of selenium nanoparticle-polyglutamic acid composite (SeNPs-PGA)

The inoculum of *B. subtilis* NT147 was prepared in sucrose yeast extract (SY) broth (20 g sucrose, 4 g yeast extract, 1 g KH_2PO_4 and 0.5 g $MgSO_4 \cdot 7H_2O$ in a liter of water, pH 6.8) and incubated at 37 ± 2 °C with shaking at 150 rpm until the OD_{600} was at 0.5). The cultured (2 % inoculum) was transferred into 50 mL SY broth and incubated at 37 ± 2 °C for 36 h with shaking at 150 rpm. Then sodium selenite was added into the culture medium at a final concentration of 2.5 mM and continue shaking until 40 h. Cells were removed by centrifugation at 8,000 rpm for 10 min. The supernatant was collected and γ-PGA was precipitated by adding 95 % cold ethanol. γ-PGA was dissolved in deionized water and freeze dried.

Quantitative analysis of selenium and selenium-enriched γ-PGA

For quantitative analysis of selenium and selenium-enriched γPGA, a sample (0.3 g) was placed into a microwave vessel. Then, 5 mL of 65 % w/w nitric acid (conc.) was added into the microwave vessel. The sample was digested using a microwave digestion system. The first digestion step was conducted at a temperature of 20 °C for 15 min. The second digestion step was also conducted at 200 °C for 15 min. After digestion, the sample was allowed to cool for 20 min. The digested sample was then transferred to a 100 mL volumetric flask and diluted to volume with deionized water. The analysis of total selenium content was performed using an inductively coupled plasma mass spectrometry (7900 ICP-MS, Agilent, USA).

Chemical synthesis of SeNPs

SeNPs were chemically synthesized by a modified method described by Ullah *et al.* [38]. Briefly, 0.25 mM ascorbic acid was added into 0.5 mM sodium selenite solution with a ratio of 1:4. The mixture was stirred at room temperature for 30 min, then the volume was adjusted to 50 mm with deionized water. SeNPs were separated by centrifugation at 10,000 rpm for 10 min and the precipitate was washed 3 times with deionized water.

Characterization of SeNPs and SeNPs-PGA

X-ray diffractometry (XRD)

An XRD (Bruker AXS model D8 discover, Worcestershire, Germany) was used to determine a crystalline structure of nanoparticles. The diffraction patterns of the sample were measured using Cu-Kα radiation (wavelength 0.154 nm) at 40 kV and 40 mA. The measurement was performed at 2θ = 5 - 40 °, step size = 0.02 °/step and a scan speed = 0.5 s/step.

Transmission electron microscopy (TEM)

The sample was dehydrated, embedded in plastic, and then sectioned into thin slices. These slices were subsequently placed onto copper grids. The sample sections were stained positively with 2 % uranyl acetate, followed by lead solution staining. The prepared samples were then analyzed using a transmission electron microscope (HT7700, Hitachi Hi-Tech Co.Ltd., Japan).

Scanning electron microscopy (FE-SEM/EDS)

The Se-PGA samples were immersed in a 2.5 % glutaraldehyde solution, followed by washing with phosphate buffer at pH 7.0. The samples were then incubated at 4 °C. Subsequently, water was removed from the cells using a series of ethyl alcohol concentrations (30, 50, 70, 80, 90, 95 and 100 %), with each concentration applied twice. The samples were then dried using a critical point dryer and coated with gold. The morphological characteristics of the samples were examined using a field emission scanning electron microscope (FESEM) model FEI Quanta 450 (Thermo

Fisher Scientific Co., Ltd., Czech Republic), operating at an acceleration voltage of 20 kV. Elemental analysis was conducted using energy-dispersive X-ray spectroscopy (EDS) (X-max, Oxford Instrument, UK).

Attenuated total reflection fourier transform infrared (ATR-FTIR) spectroscopy

The sample was prepared in a KBr disc format by mixing 2 mg of the sample with 80 - 100 mg of KBr powder and grinding them together. The mixture was then pressed into a disc using a hydraulic press. The prepared KBr disc was analyzed using the ATR-FTIR spectroscopy (Vertex 70, Bruker, Germany), scanning in the range of 400 - 4,000 cm^{-1} with a resolution of 4 cm^{-1}.

Laser scattering particle size distribution analyzer

Bacterial cells were lysed by using an ultra-sonicate probe (Vibra-cell VCX 750, Sonics & Materials, Inc., USA) at 50 % duty cycle, and 160 W for 3 min. The sample was approximately diluted with 2 - 3 drops of the sample into 15 mL of distilled water then it was dropped into a quartz cell and analyzed by the laser scattering particle size distribution analyzer (LA-950 model, Horiba, USA).

Quantitative analysis of γ-PGA

Production of γ-PGA can increase culture broth viscosity. Thus, the culture broth was measured for its viscosity by using a viscometer (Brookfield, LVDV-2T model, China) with a spindle suitable for samples with a viscosity greater than 15 Cp. The measurement was conducted at a speed of 150 rpm for 5 min. The standard curve was done by using 50 - 1,000 ppm of high molecular weight γ-PGA (> 200 KDa) solution.

Antifungal activity of Se-PGA

The fungus *Colletotrichum* sp. was cultured on potato dextrose agar (PDA) for 7 days. PDA supplemented with Se-PGA at concentrations of 500, 1,000, 1,500 and 2,000 mg/L was prepared, and the medium was sterilized at 121 °C for 15 min. Following sterilization, 0.02 % streptomycin was added to the medium before pouring it into Petri dishes. For the positive control, 0.5 % carbendazim and 0.02 % streptomycin were included, while the negative control consisted of the PDA without any antifungal agents. Fungal mycelial was obtained from 7-day-old cultures and placed onto the Se-PGA supplemented PDA. After incubation at 25 ± 2 °C for 7 days, the radial growth of the fungus on the PDA was measured. The percentage of inhibition was calculated based on the formula described by Joshi *et al.* [39]:

$$\text{Percentage inhibition} = \{(Rc - Rt)/Rc\} \times 100$$

where, Rc is the radial growth of the control and Rt is the radial growth of the treatment.

Statistical analysis

Statistical analysis was carried out using SPSS 16.0 (SPSS Inc., Illinois, USA). Data were analyzed using 1-way analysis of variance followed by Duncan's multiple range test at the 0.05 level of probability.

Results and discussion

Growth, selenite reduction and γ-PGA production of *B. subtilis* NT147

The effect of Na_2SeO_3 on the growth and production of γ-polyglutamic acid (γ-PGA) in *B. subtilis* NT147 was investigated in red colonies that lost their mucoid appearance. Notably, growth significantly decreased when 35 mM Na_2SeO_3 was applied. As the concentration of selenite increased on LB agar plates, bacterial growth diminished. In LB broth experiments, Na_2SeO_3 was added at concentrations ranging from 0.5 to 2.5 mM. The culture supplemented with 0.5 mM Na_2SeO_3 exhibited growth comparable to that of the control (**Figure 1(A)**), which prompted further examination of selenium production at this concentration. During the initial stages of incubation, the culture medium became cloudy yellow, transitioning to a pinkish hue at 6 h, and ultimately turning red by 9 h, suggesting the formation of selenium element (S^0). The selenium content in the biomass increased dramatically from 0.150 ± 0.042 g/kg dry weight (DW) to 11.3 ± 0.24 g/kg DW after 6 h of incubation, while selenium levels in the culture medium remained low (**Figure 1(B)**). The decrease of Se in bacterial cells after 6 h may be related to cell lysis following exposure to Na_2SeO_3. A reduction of Se in the cells of *Bacillus*

niabensis OAB2 was observed as well [40]. The experimental results align with previous research indicating that different microbial species exhibit varying levels of tolerance to selenite when supplemented in growth media. *Rahnella aquatilis* HX2 has a minimal inhibitory concentration (MIC) for selenite of 85 mM [3], whereas the growth of *Delftia* sp. decreases by 3-fold when cultured in media supplemented with 2.5 mM of selenite [7]. The growth *Bacillus* sp. in 3 mM selenite treatment was higher than other treatments (5 - 50 mM), indicating that the high concentration of selenite inhibited the proliferation of bacteria [18]. Selenite (Se(IV)) is generally toxic to microbial cells, necessitating the development of mechanisms by which microorganisms mitigate its toxicity, such as the reduction of selenite to elemental selenium, which is red in color. The production of biogenic selenium nanoparticles (SeNPs) can be facilitated by bacteria in the presence of selenite or selenate. Various metabolic pathways have been proposed for the reduction of selenite by microorganisms. Under aerobic conditions, selenite can be reduced to SeNPs through the action of fumarate reductase and selenite reductase [19]. One of the most well-established mechanisms of selenium reduction involves thiol compounds, where reduced thioredoxin interacts with selenodiglutathione, resulting in the oxidation of thioredoxin, the reduction of glutathione, and the formation of selenopersulfide anion, ultimately leading to the release of elemental sulfur (S^0) [41]. Multiple mechanisms can be engaged in selenite reduction within a single bacterial strain, contingent upon the concentration of selenite to which it is exposed [42]. Not only growth inhibition but selenite also reduced γ-PGA synthesis. The highest γ-PGA amount produced in SY medium at 24 h was 4.82 ± 0.05 mg/L; however, γ-PGA content trended to decrease at 36 and 48 h (**Figure 1(C)**), suggesting extracellular γ-glutamyl hydrolases hydrolyzed a high molecular weight γ-PGA to lower size resulting in reduction of culture medium viscosity [29]. Whereas, the production of γ-PGA was markedly inhibited when cells were grown in SY medium supplemented with 0.5 mM Na_2SeO_3, indicating that selenite has an inhibitory effect on the production of γ-PGA. This finding is consistent with the observed reduction in the mucoid appearance of colonies on LB agar plates containing selenite. Adding of selenite (20 μg/mL) with inoculation in the medium resulted in no biomass and exopolysaccharide production of *Pseudomonas* PT-8 [22].

Morphology of SeNPs

Transmission Electron Microscopy (TEM) was utilized to examine the morphology and size of selenium nanoparticles (SeNPs) synthesized by *B. subtilis* NT147 (**Figure 2**). Compared to the control (**Figures 2(A) - 2(B)**), bacterial cells cultivated in LB medium augmented with 0.5 mM Na_2SeO_3 demonstrated the presence of selenium particles predominantly within the cells at 12 h (**Figure 2(C)**), with some of the particles released outside of cells at 24 h due to cell lysis (**Figure 2(D)**). The TEM image clearly indicates the presence of spherical SeNPs, with an increase in particle size observed after 24 h of cell growth. The average diameter of Se particles detected in bacterial cells was 92.1 ± 33.38 and 335.2 ± 84.1 nm at 12 and 24 h, respectively. The analysis patterns from the Laser Scattering Particle Size Distribution Analyzer showed that cultivation time obviously affected the size of SeNPs (**Figure 3**). SeNPs were synthesized during the initial growth phase (6 - 12 h). SeNPs demonstrated poor dispersion and a tendency to congregate, increasing particle sizes at 18 - 24 h. SeNPs were found at 6 and 12 h, ranging from 200 - 600 and 200 - 1,000 nm, respectively. These results correspond with the TEM images (**Figures 2(C) - 2(D)**), indicating that the size of SeNPs increases with incubation time. The larger average size of selenium nanoparticles (SeNPs) observed using the Laser Scattering Particle Size Distribution Analyzer may result from the aggregation of SeNPs in the liquid solution during sample preparation, as well as from their binding to macromolecules such as proteins released during cell lysis [41]. The particle size of SeNPs synthesis by microorganisms is varied depending on strains and culture conditions. *Bacillus paramycoides* SP3 isolated from coal mine wash water synthesized spherical SeNPs within the cells, with particle sizes ranging from 120 to 170 nm [23]. *Bacillus amyloliquefaciens* can reduce selenite to spherical SeNPS ranging from 45.4 to 68.3 nm [43]. SeNPs synthesized by *B. licheniformis* F1 exhibited a spherical morphology, with average diameters ranging from 110 to 170 nm. In contrast, the remaining 2 *Enterococcus*

strains were responsible for the production of volatile selenium compounds, specificaly dimethyl-diselenide [44,45]. The absorption of nanoparticles (NPs) with sizes smaller than 100 nm in the gastrointestinal tract is significantly greater, being 15 to 250 times higher compared to that of larger NPs [46]. Our findings indicate that the size of selenium nanoparticles (SeNPs) was influenced by the cultivation time. During the exponential phase of biosynthesis, SeNPs with an average size of 92.1 ± 33.38 nm were produced. Additionally, *Bacillus subtilis* DA20 generated spherical SeNPs with sizes ranging from 20 to 65 nm. When used as a dietary supplement in broiler diets, these SeNPs significantly enhanced chick body weight and reduced the feed conversion ratio [47]. Therefore, based on the properties and size of the selenium nanoparticles synthesized by *B. subtilis* NT147, these nanoparticles may have potential medical or agricultural applications, such as in supplements for humans or animals. This is due to the fact that *B. subtilis* is a bacterium isolated from food sources and is safe for consumption.

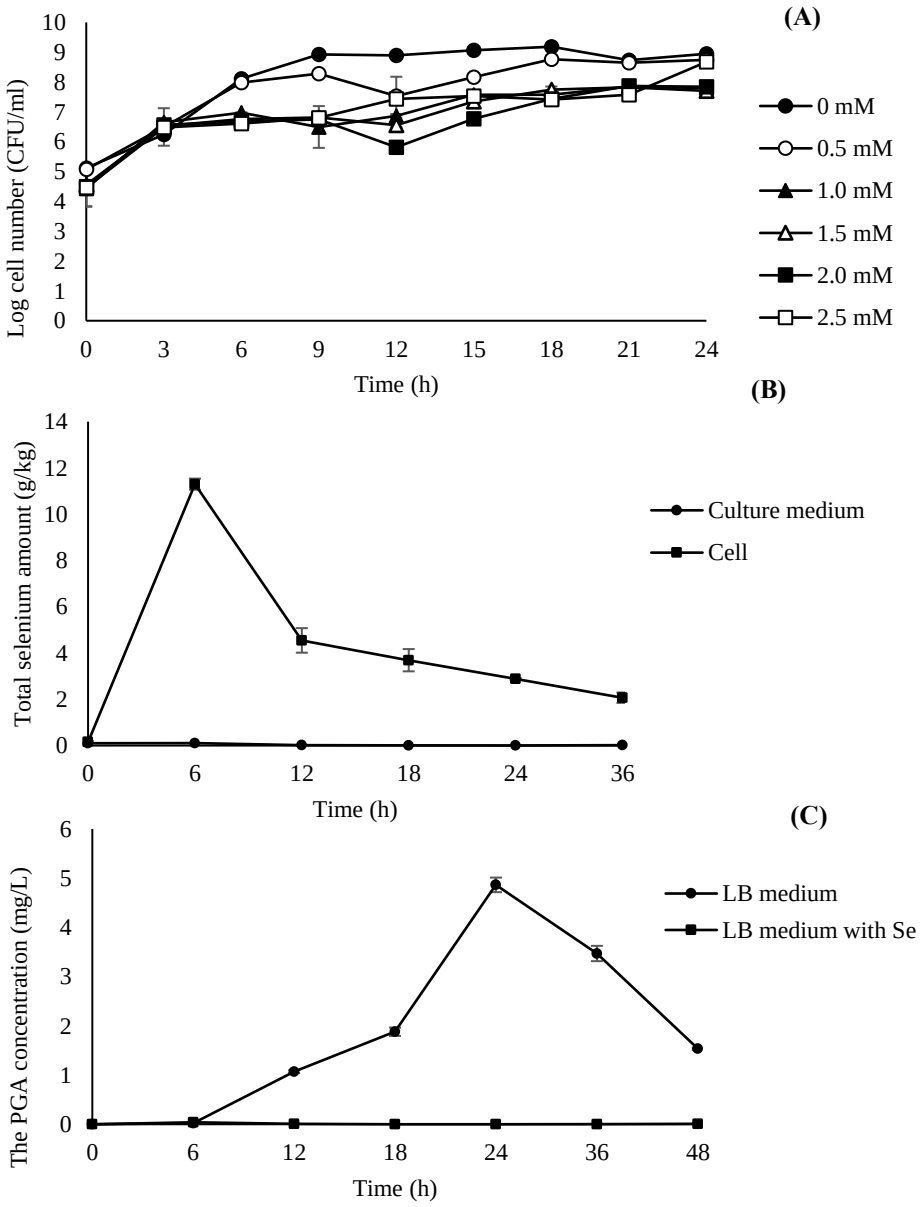

Figure 1 Growth, reduction of selenite and γ-PGA production of *B. subtilis* NT147 cultivated in medium supplemented with Na_2SeO_4: A) growth in LB broth containing 0.5 - 2.5 mM Na_2SeO_3; B) amount of selenium in cells and culture medium and; C) γ-PGA production of *B. subtilis* NT147 grown in SY medium containing 0.5 mM Na_2SeO_3.

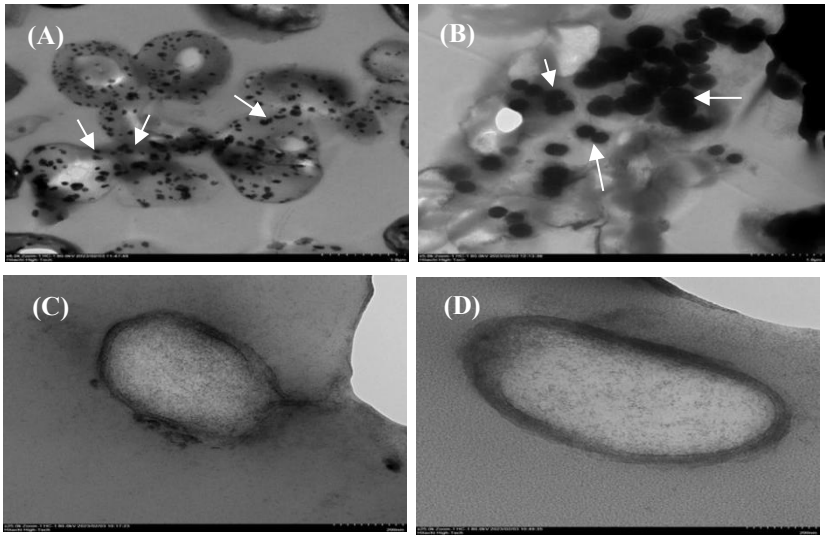

Figure 2 Transmission electron microscopy of selenium in cell of *B. subtilis* NT147 depicting spherical nanoparticles (SeNPs): (A) 12-h cell grown in LB broth without Na_2SeO_3, (B) 12-h cell grown in LB broth without Na_2SeO_3, (C) 12-h cell grown in LB broth with Na_2SeO_3 and (D) 12-h cell grown in LB broth with Na_2SeO_3.

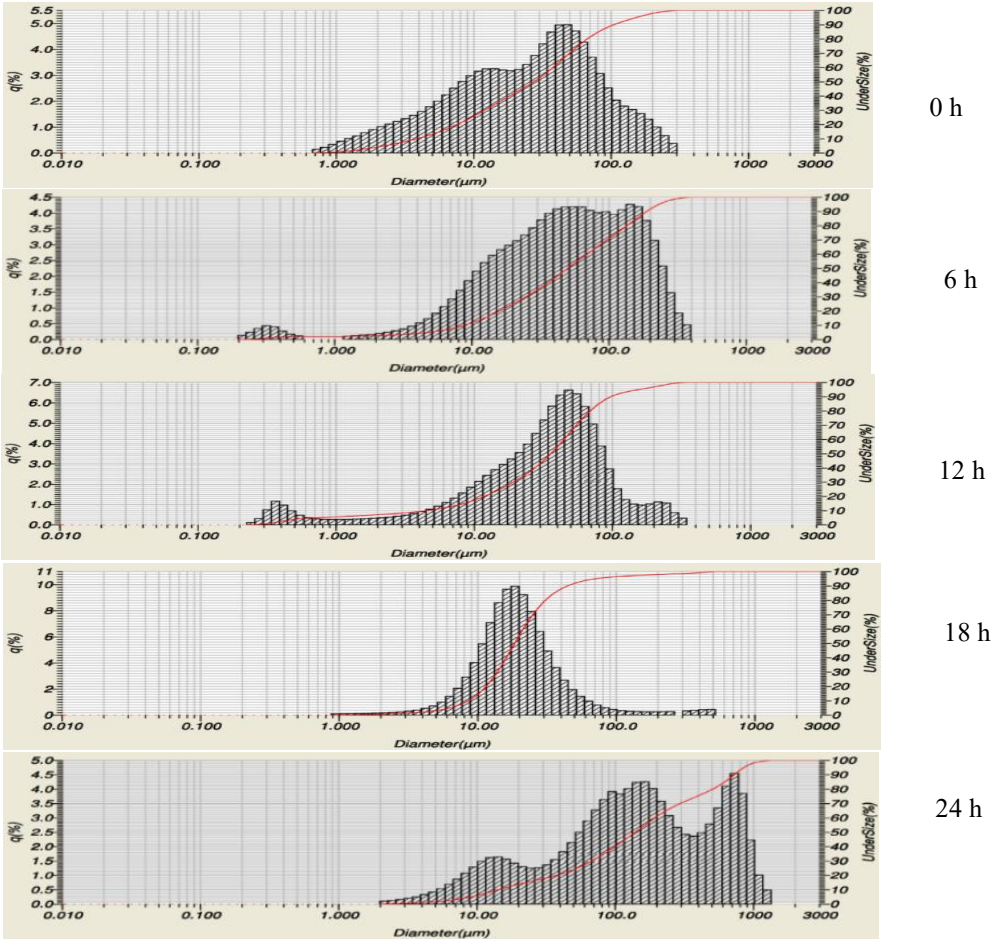

Figure 3 The distribution and size of SeNPs analyzed by laser scattering particle size analyzer.

Production and characterization of Se-PGA

Due to the inhibitory effect of Na_2SeO_3 on γ-PGA production when added at the beginning of growth, γ-PGA was produced in sucrose yeast extract (SY) medium, with bacterial cultures grown for 36 h to maximize γ-PGA yield. Following this, 2.5 mM of

Na_2SeO_3 was introduced, and the culture was continuously shaken for an additional 4 h. During this period, the suspension turned red. After the cells were removed, γ-PGA was precipitated, resulting in the formation of pinkish-red γ-PGA (**Figure 4(A)**). The amount of Se in γ-PGA was 2.007 g/kg. The production of γ-PGA is influenced by the type of culture medium, cultivation time and the specific strain used. Two types of γ-PGA-producing strains have been identified: Glutamate-dependent strains, which produce high amounts of γ-PGA when L-glutamate is supplemented in the culture medium and glutamate-independent strains, which produce γ-PGA through the tricarboxylic acid cycle. γ-PGA production reaches its maximum during the stationary phase [29]. *Bacillus subtilis* NT147, a glutamate-independent strain, can utilize sucrose as a substrate for γ-PGA production, making it a cost-effective option for large-scale production using inexpensive substrates. The biosynthesis of selenium-enriched EPS by *Pseudomonas* PT-8 through submerged fermentation demonstrated that the addition of Na_2SeO_3 after 24 h did not impact cell growth. The optimal conditions for selenium-enriched EPS required the addition of 20 mg/L selenite to the medium at the 6 h of fermentation [22]. In this experiment, SEM image showed the dispersion of spherical SeNPs within γ-PGA (**Figure 4(B)**). The existence of Se was confirmed by EDS, and additional elements including as carbon, nitrogen, and oxygen were detected, confirming the presence of γ-PGA (**Figure 4(C)**). Attenuated Total Reflection Fourier Transform Infrared (ATR-FTIR) spectroscopy was employed to evaluate the chemical characteristics of Se-PGA by examining important functional groups throughout the wavenumber range of 4,000 - 600 cm^{-1} (**Figure 5(A)**). A peak corresponding to γ-PGA was observed at 3,268 cm^{-1} (-OH stretching), 1,581 cm^{-1} (C=O of carbonyl) and 1,400 - 1,000 cm^{-1} (C-O stretching, C-C stretching and C-O-C stretching), which is consistent with findings by [48]. The γ-PGA produced by *Bacillus velezensis* VCN56 showed a peak at 3,407 cm^{-1} (-OH stretching), indicating the presence of proteins and amino acids. Additionally, peaks at 1,658 and 1,453 cm^{-1} (C=O stretching) were observed. For Se-PGA, peaks were observed at 2,923 cm^{-1} (CH_2 stretching), 1,623 cm^{-1} (possibly indicating an amine group), 1,456 cm^{-1} (C-C stretching) and 1,053 cm^{-1} (alcoholic group), which align with the findings of Wang *et al.* [53]. SeNPs synthesized from ascorbic acid, peaks were detected at 3,228 cm^{-1} (-OH stretching) and 1,618 cm^{-1} (C-H stretching), which are close to those reported by Siddique *et al.* [49]. Additionally, peaks at 773 and 774 cm^{-1} were observed for both the chemically synthesized SeNPs and Se-PGA, corresponding to SeO stretching and bending vibrations, possibly due to the interaction between the selenium nanoparticles and the carbonyl group of ascorbic acid and γ-PGA [50]. These functional groups suggest the presence of various functional entities, which may play a role in the reduction and stabilization of selenium nanoparticles [51]. SeNPs synthesized by *B. subtilis* MKUST-03, found a peak at 3,454 cm^{-1} for the -OH stretching group in EPS, with a slight shift to 3,425 cm^{-1} for the nanoparticle-EPS interaction, suggesting interference in nanoparticle aggregation [10]. SeNPs synthesized by bacteria may be coated with biomolecules such as proteins, polysaccharides and lipids, particularly proteins on the nanoparticle surface. The protein structures may differ from those in natural cells, with characteristic peaks in the range of 1,620 - 1,680 cm^{-1}, corresponding to the amide I group [52]. The stabilization of SeNPs by the γ-PGA structure has been suggested as illustrated in **Figure 5(B)**. X-ray diffraction (XRD) analysis (**Figure 6**) was conducted in the 2θ range of 5 to 40 °. The highest peaks for chemically synthesized selenium nanoparticles (**Figure 6(A)**) were observed at 23.78, 29.91, 41.54, 43.93, 45.71, 51.99 and 52.003 °. In contrast, the XRD peaks for Se-PGA were found at 23.98, 30.06 and 43.93 °, corresponding to the planes (100), (101), (102), (111), (201) and (211) (**Figure 6(B)**), which aligns with the findings of Siddique *et al.* [49]. Furthermore, the XRD analysis of SeNPs revealed significant peaks at 23.9, 29.8, 43.7, 45.7, 51.9 and 68.4 °, corresponding to the same crystallographic planes (100), (101), (102), (111), (201) and (211) as reported by Ramachandran *et al.* [10]; Wang *et al.* [53]. The study investigated the effects of bacterial exopolysaccharides (EPS) on the structure and biological properties of selenium nanoparticles and identified peaks at 2θ values of 30, 41.7, 44, 45.7, 52, 56.4, 62.2, 65.5 and 68.4 °. Notably, the peaks of the selenium nanoparticles and EPS coincided; however,

background noise was present, potentially due to the influence of EPS.

Modulating of microbial biopolymer such as EPS with nanoparticles is an emerging application of nanotechnology due to the enhancement of soil fertility, encouragement of nutrient uptake, and plant growth in agriculture. The synthesis of selenium nanoparticles in conjunction with biopolymers is typically performed by first synthesizing the polymer and then mixing it with selenium or separately synthesized selenium nanoparticles. Mycogenic SeNPs synthesized by culture filtrate of *Serendioitia indica* was purified and mixed with EPS produced by *B. subtilis*. There is limited research reporting on the simultaneous synthesis of polymers integrated with selenium nanoparticles. The production method using bacterial fermentation may prove to be more straightforward and cost-effective. Our findings demonstrated the successful dispersion of SeNPs within a γ-PGA matrix, presenting a potential 1-step method for synthesizing SeNPs incorporated with an edible biopolymer by bacteria. γ-PGA is water-soluble and exhibits high thermal stability. The melting point (Tm) and decomposition temperature (Td) of γ-PGA have been reported to be 219 and 223 °C, respectively [54]. γ-PGA has also been used to modify other biopolymers, such as bacterial cellulose (BC) [55]. Additionally, γ-PGA has been combined with chitosan using an *in situ* approach to create wound dressing materials. The resulting BC/γ-PGA/chitosan composite displayed antibacterial properties, biocompatibility with animal cells and enhanced wound healing [56]. When BC is incorporated into a γ-PGA hydrogel matrix, it demonstrates excellent cytocompatibility, making it highly suitable for biomaterial applications [57]. Therefore, incorporating SeNPs into γ-PGA enhances the value of the composite, and SeNPs-PGA exhibits considerable potential for a variety of applications, including medical, dietary and feed-related uses.

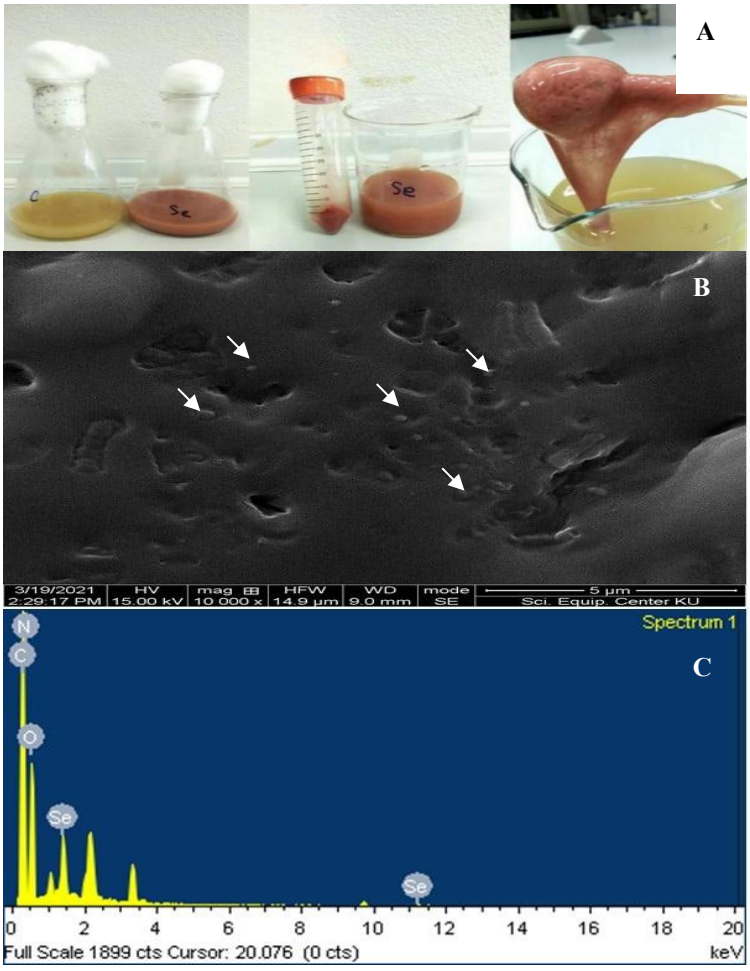

Figure 4 Se-PGA: (A) Se-PGA produced from *B. subtilis* NT147; (B) FE-SEM image of Se-PGA and (C) analysis of elements appeared in Se-PGA by EDS.

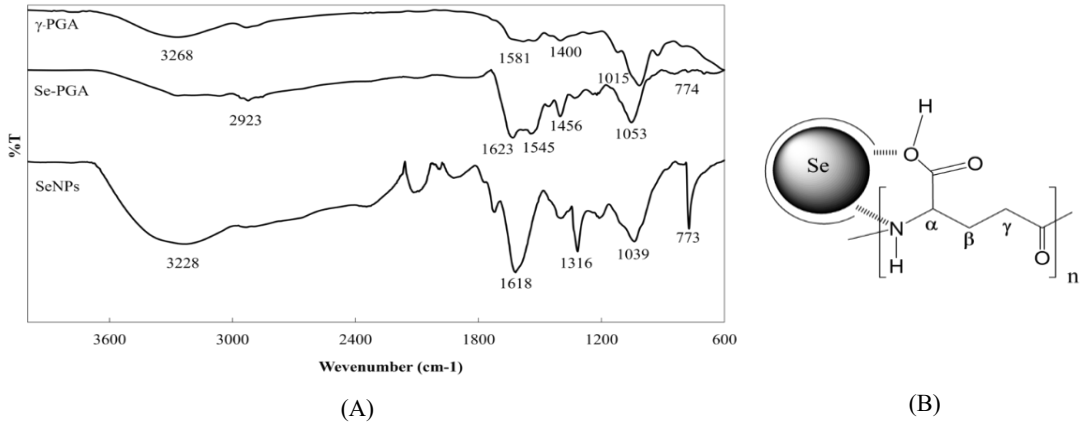

(A) (B)

Figure 5 ATR-FTIR analysis: (A) spectra of γ-PGA, chemical synthesized SeNPs and Se-PGA and (B) SeNPs stabilized with γ-PGA.

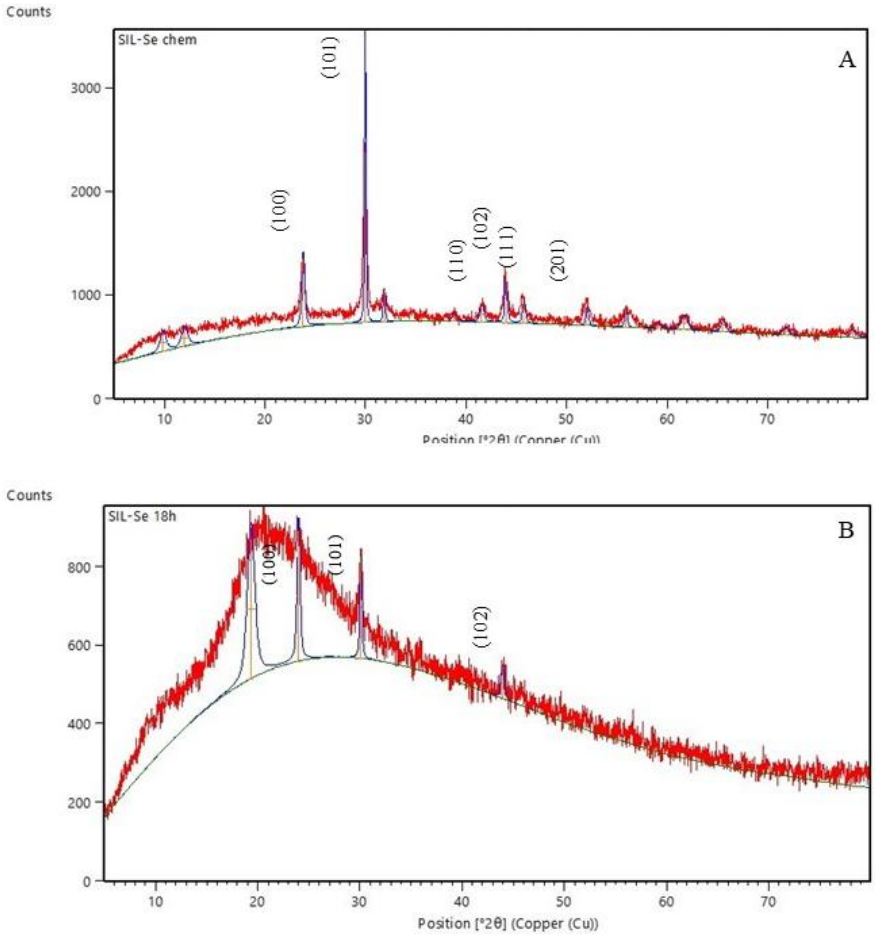

Figure 6 XRD analysis: (A) Se synthesized through chemical methods and (B) Se-PGA synthesized by *B. subtilis*

Antifungal activity

The antifungal efficacy of Se-PGA was evaluated against *Colletotrichum* sp., a phytopathogenic fungus. The antifungal activity exhibited an increasing trend, achieving 8.75, 12.23, 15.82 and 17.96 % inhibition at concentrations of 500, 1,000, 1,500 and 2,000 µg/mL of Se-PGA, respectively as shown in **Table 1**. The relatively low antifungal activity of Se-PGA may be

associated with the selenium content present on the γ-PGA and the amount of bioactive selenium that is effective against fungal pathogens. Several reports have demostrated the antifugal activity of biogenic SeNPs. Se levels (0.1 and 0.5 mg/kg) applied in soil decreased the lesion diameter and incidence of *S. sclerotiorum* in rape leaves [58]. SeNPs derived from *Desmonostoc alborizicum* at concentrations of 5 and 10 µg/mL exhibited inhibitory zones of 10.66 and 14.33 mm against *C. gloeosporioides*, respectively [26,59]. Chemically synthesized selenium nanocomposites (SeNC) utilizing natural polysaccharide matrices such as arabinogalactan, starch and κ-carrageenan effectively inhibited the phytopathogen *Phytophthora cactorum*. Among these, the arabinogalactan-based SeNC and κ-carrageenan-based SeNC demonstrated the highest levels of fungal growth inhibition, achieving up to 60 % (at 300 µg/mL) and 49 % (at 234 µg/mL), respectively [60]. Therefore, the effectiveness of SeNPs in inhibiting plant pathogenic fungi varies with particle size and stability. Additionally, different fungal species exhibit varying levels of resistance to SeNPs, which may be related to their distinct metabolic processes and detoxification mechanisms. The exact mechanism by which SeNPs inhibit fungal growth remains uncertain. However, evidence suggests that inorganic selenium, along with organic diselenides and methyl-selenides, can disrupt the membrane proteins of pathogens by generating free radicals through reactions with the thiol groups of these proteins [18,61]. SeNPs have the potential to penetrate the cell membrane and disrupt its integrity, which can result in the leakage of essential cellular components and ultimately lead to cell death. In a study by Shahbaz *et al.* [62], inhibition of *Fusarium mangiferae* conidial germination was observed when fungal suspension was treated with 300 µg/mL SeNPs, compared to the control group, where 100 % germination occurred. The antifungal mechanism of SeNP/PVP/Nystatin nanoconjugates was further investigated by measuring the transcript levels of key genes involved in morphogenesis and biofilm formation in *Candida albicans* using RT-PCR. Specifically, the RAS/cAMP/PKA signaling pathway, which is critical for the yeast-to-hyphae transition and biofilm formation, was examined. The results indicated that genes associated with hyphal growth and biofilm formation were downregulated [63].

Table 1 Inhibition of *Colletotrichum* sp. by Se-PGA produced by *B. subtilis* NT147.

	Percentage of inhibition (%)
Cabendazim 5 mg/L	76.15 ± 1.06^{a}
SeNPs-PGA 500 mg/L	8.75 ± 1.21^{e}
SeNPs-PGA 1,000 mg/L	12.23 ± 15.9^{d}
SeNPs-PGA 1,500 mg/L	15.82 ± 0.58^{c}
SeNPs-PGA 2,000 mg/L	17.96 ± 0.70^{b}

Different superscripts in a column differ significantly ($p < 0.05$) according to Duncan's multiple range test.

Although the antifungal activity observed in this study is not particularly high, this work demonstrates the potential for producing Se-enriched γ-PGA, which can bse achieved simultaneously through a fermentation process. Additionally, this research presents the synthesis of SeNPs in conjunction with polyamino acid polymers, distinguishing it from numerous other studies that primarily focus on exopolysaccharides (EPS). However, further investigation is needed to determine the optimal conditions for maximizing the yield of selenium and γ-PGA. Additionally, the appropriate size of γ-PGA, which may influence the efficacy and biological activity of Se-PGA, remains an important area for further research and development. Research into other agricultural applications, such as seed coating or fertilizers, represents another avenue for utilizing Se-PGA. However, further studies are needed to evaluate its effectiveness in these contexts. The beneficial characteristics of selenium nanoparticles (SeNPs) and γ-PGA indicate prospective uses of SeNPs and Se-PGA in

industrial, agricultural and health areas, along with their role in promoting green and environmentally sustainable technologies.

Conclusions

In conclusion, the synthesis of selenium nanoparticles (SeNPs) and selenium-enriched γ-polyglutamic acid (Se-PGA) by *Bacillus subtilis* NT147 was investigated. The study demonstrated that organic SeNPs were synthesized intracellularly. The SeNPs were spherical in shape, with an average size of 335.2 ± 84.1 nm at 24 h, although the particle distribution became less uniform after 18 h of cultivation. Selenium-enriched PGA was produced using a submerged culture method. The addition of Na_2SeO_3 during the stationary phase of bacterial growth resulted in the formation of Se-PGA, with a selenium content of 2.007 g/kg. Characterization of Se-PGA revealed that SeNPs were spherical and dispersed within the γ-PGA matrix. Furthermore, Se-PGA exhibited fungal inhibitory activity. These findings demonstrate the potential of producing Se-PGA via fermentation; however, further optimization and studies are required to improve the production process and enhance its biological activity. Ultimately, Se-PGA production through fermentation holds promise for large-scale, cost-effective production, with potential applications in agriculture, animal feeds and dietary supplements.

Acknowledgments

This research is supported in part by the Graduate Program Scholarship from The Graduate School, Kasetsart University, Thailand.

References

[1] J Sarkar, D Mridha, MA Davoodbasha, J Banerjee, S Chanda, K Ray, T Roychowdhury, K Acharya and J Sarkar. A state-of-the-art systemic review on selenium nanoparticles: Mechanisms and factors influencing biogenesis and its potential applications. *Biological Trace Element Research* 2023; **201(10)**, 5000-5036.

[2] X Nie, X Yang, J He, P Liu, H Shi, T Wang and D Zhang. Bioconversion of inorganic selenium to less toxic selenium forms by microbes: A review. *Frontiers in Bioengineering and Biotechnology* 2023; **11**, 1167123.

[3] Y Zhu, B Ren, H Li, Z Lin, G Bañuelos, L Li, G Zhao and Y Guo. Biosynthesis of selenium nanoparticles and effects of selenite, selenate, and selenomethionine on cell growth and morphology in *Rahnella aquatilis* HX2. *Applied Microbiology and Biotechnology* 2018; **102(14)**, 6191-6205.

[4] R Sowmya, SKR Namasivayam and SK Shree. A critical review on nano-selenium based materials: Synthesis, biomedicine applications and biocompatibility assessment. *Journal of Inorganic and Organometallic Polymers and Materials* 2024; **34**, 3037-3055.

[5] DM Cruz, G Mi and TJ Webster. Synthesis and characterization of biogenic selenium nanoparticles with antimicrobial properties made by *Staphylococcus aureus*, methicillin-resistant *Staphylococcus aureus* (MRSA), *Escherichia coli*, and *Pseudomonas aeruginosa*. *Journal of Biomedical Materials Research Part A* 2018; **106(5)**, 1400-1412.

[6] JJO Garza-García, JA Hernández-Díaz, JM León-Morales, G Velázquez-Juárez, A Zamudio-Ojeda, J Arratia-Quijada, OK Reyes-Maldonado, JC López-Velázquez1 and S García-Morales. Selenium nanoparticles based on *Amphipterygium glaucum* extract with antibacterial, antioxidant, and plant biostimulant properties. *Journal of Nanobiotechnology* 2023; **21(1)**, 252.

[7] M Pescuma, F Aparicio, RD Zysler, E Lima, C Zapata, JA Marfetán, ML Vélez and OF Ordoñez. Biogenic selenium nanoparticles with antifungal activity against the wood-rotting fungus *Oligoporus pelliculosus*. *Biotechnology Reports* 2023; **37**, e00787.

[8] G Murugesan, K Nagaraj, D Sunmathi and K Subramani. Methods involved in the synthesis of selenium nanoparticles and their different applications - a review. *European Journal of Biomedical and Pharmaceutical sciences* 2019; **6(4)**, 189-194.

[9] AE Abdelhamid, EH Ahmed, HM Awad and MMH Ayoub. Synthesis and cytotoxic activities of selenium nanoparticles incorporated nano-chitosan. *Polymer Bulletin* 2024; **81(2)**, 1421-1437.

[10] T Ramachandran, D Manoharan, S Natesan, SK Rajaram, P Karuppiah, MR Shaik, M Khan and B Shaik. Synthesis and structural characterization of selenium nanoparticles - *Bacillus* sp. MKUST-01 exopolysaccharide (SeNPs-EPS) conjugate for biomedical applications. *Biomedicines* 2023; **11(9)**, 2520.

[11] P Concórdio-Reis, AC Macedo, M Cardeira, X Moppert, J Guézennec, C Sevrin, C Grandfils, AT Serra and F Freitas. Selenium bio-nanocomposite based on *Alteromonas macleodii* Mo169 exopolysaccharide: Synthesis, characterization, and *in vitro* antioxidant activity. *Bioengineering* 2023; **10(2)**, 193.

[12] E Khaledizade, F Tafvizi and P Jafari. Anti-breast cancer activity of biosynthesized selenium nanoparticles using *Bacillus coagulans* supernatant. *Journal of Trace Elements in Medicine and Biology* 2024; **82**, 127357.

[13] J Song, J Zhou, X Li, P Li, G Tian, C Zhang and D Zhou. Nano-selenium stablilized by Konjac Glucommannan and its biological activity *in vitro*. *LWT* 2022; **161**, 113289.

[14] KE Yunusov, AA Sarymsakov, JZO Jalilov and AA Atakhanov. Physicochemical properties and antimicrobial activity of nanocomposite films based on carboxymethylcellulose and silver nanoparticles. *Polymers for Advanced Technologies* 2022; **32(4)**, 1822-1830.

[15] W Fuangchoonuch, K Chompoonuch, K Amprayn, O Chunhachart, S Prateepchinda, S Benjautthaya, W Laosripaiboon, S Jarussophon and N Jaratsophon. Characterization, selenium accumulation and their antioxidant activity with different forms of coated selenium nanoparticles in sunflower sprout. Chemistry for catalyzing sustainability and prosperity. *In*: Proceedings of the Pure and Applied Chemistry International Conference, Nonthaburi, Thailand. 2020, p. 127-132.

[16] EO Mikhailova. Selenium nanoparticles: Green synthesis and biomedical application. *Molecules* 2023; **28(24)**, 8125.

[17] S Zheng, J Su, L Wang, R Yao, D Wang, Y Deng, R Wang, G Wang and C Rensing. Selenite reduction by the obligate aerobic bacterium *Comamonas testosteroni* S44 isolated from a metal-contaminated soil. *BMC Microbiology* 2014; **14(1)**, 204.

[18] Y Yang, J Jing, S Fan, Z Chen and Y Qu. Unraveling the molecular mechanisms of selenite reduction: Transcriptomic analysis of *Bacillus* reveals the key role of sulfur assimilation. *Biotechnology Letters* 2023; **45(11)**, 1513-1520.

[19] D Wang, C Rensing and S Zheng. Microbial reduction and resistance to selenium: Mechanisms, applications and prospects. *Journal of Hazardous Materials* 2022; **421**, 126684.

[20] A Kumar, B Prasad, J Manjhi and KS Prasad. Antioxidant activity of selenium nanoparticles biosynthesized using a cell-free extract of *Geobacillus*. *Toxicological and Environmental Chemistry* 2020; **102(10)**, 556-567.

[21] Y Duan, M Li, S Zhang, Y Wang, J Deng, Q Wang, T Yi, X Dong, S Cheng, Y He, C Gao and Z Wang. Highly efficient biotransformation and production of selenium nanoparticles and polysaccharides using potential probiotic *Bacillus subtilis* T5. *Metabolites* 2022; **12(12)**, 1204.

[22] S Ye, J Zhang, Z Liu, Y Zhang, J Li and YO Li. Biosynthesis of selenium rich exopolysaccharide (Se-EPS) by *Pseudomonas* PT-8 and characterization of its antioxidant activities. *Carbohydrate Polymers* 2016; **142**, 230-239.

[23] SN Borah, L Goswami, S Sen, D Sachan, H Sarma, M Montes, JR Peralta-Videa, K Pakshirajan and M Narayan. Selenite bioreduction and biosynthesis of selenium nanoparticles by *Bacillus paramycoides* SP3 isolated from coal mine overburden leachate. *Environmental Pollution* 2021; **285**, 117519.

[24] S Bharathi, S Kumaran, G Suresh, M Ramesh, V Thangamani, SR Pugazhvendan and K Sathiyamurthy. Extracellular synthesis of nanoselenium from fresh water bacteria *Bacillus* sp., and its validation of antibacterial and cytotoxic potential. *Biocatalysis and Agricultural Biotechnology* 2020; **27**, 101655.

[25] P Liu, H Long, H Cheng, M Liang, Z Liu, Z Han, Z Guo, H Shi, M Sun and S He. Highly-efficient synthesis of biogenic selenium nanoparticles by *Bacillus paramycoides* and their antibacterial and antioxidant activities. *Frontiers in Bioengineering and Biotechnology* 2023; **11**, 1227619.

[26] AH Hashem, AM Abdelaziz, AA Askar, HM Fouda, AMA Khalil, KA Abd-Elsalam and MM Khaleil. *Bacillus megaterium*-mediated synthesis of selenium nanoparticles and their antifungal activity against *Rhizoctonia solani* in Faba Bean plants. *Journal of Fungi* 2021; **7(3)**, 195.

[27] X Yong, W Raza, G Yu, W Ran, Q Shen and X Yang. Optimization of the production of poly-γ-glutamic acid by *Bacillus amyloliquefaciens* C1 in solid-state fermentation using dairy manure compost and monosodium glutamate production residues as basic substrates. *Bioresource Technology* 2011; **102(16)**, 7548-7554.

[28] AD Cesaro, SBD Silva, VZD Silva and MAZ Ayub. Physico-chemical and rheological characterization of poly-gamma-glutamic acid produced by a new strain of *Bacillus subtilis*. *European Polymer Journal* 2014; **57**, 91-98.

[29] K Elbanna, FS Alsulami, LA Neyaz and HH Abulreesh. Poly (γ) glutamic acid: A unique microbial biopolymer with diverse commercial applicability. *Frontiers in Microbiology* 2024; **15**, 1348411.

[30] G Wang, Q Liu, Y Wang, J Li, Y Chen, Q Wen, D Zheng, W Kang and H Quan. The application and functional progress of γ-poly-glutamic acid in food: A mini-review. *Current Pharmaceutical Design* 2020; **26(41)**, 5347-5352.

[31] SB Park, MH Sung, H Uyama and DK Han. Poly (glutamic acid): Production, composites, and medical applications of the next-generation biopolymer. *Progress in Polymer Science* 2021; **113**, 101341.

[32] N Ngearnpat, O Chunhachart, N Kotabin and K Issakul. Comparative assessment of gamma-polyglutamic acid and *Bacillus subtilis* cells as biostimulants to improve rice growth and soil quality. *Journal of Ecological Engineering* 2023; **24(12)**, 46-59.

[33] Z Xu, P Lei, X Feng, S Li and H Xu. Analysis of the metabolic pathways affected by poly-γ-glutamicacid in *Arabidopsis thaliana* based on genechip microarray. *Journal of Agricultural and Food Chemistry* 2016; **64(32)**, 6257-6266.

[34] H Ma, P Li, N Xiao and T Xia. Poly-γ-glutamic acid promoted maize root development by affecting auxin signaling pathway and the abundance and diversity of rhizosphere microbial community. *BMC Plant Biology* 2022; **22(1)**, 521.

[35] H El-Ramady, N Abdalla, HS Taha, T Alshaal, A El-Henawy, SE-DA Faizy, MS Shams, SM Youssef, T Shalaby, Y Bayoumi, N Elhawat, S Shehata, A Sztrik, J Prokisch, M Fári, É Domokos-Szabolcsy, EA Pilon-Smits, D Selmar, S Haneklaus and E Schnug. Selenium and nano-selenium in plant nutrition. *Environmental Chemistry Letters* 2016; **14**, 123-147.

[36] AA Nagdalian, AV Blinov, SA Siddiqui, AA Gvozdenko, AB Golik, DG Maglakelidze, IV Rzhepakovsky, MY Kukharuk, SI Piskov, MB Rebezov and MA Shah. Effect of selenium nanoparticles on biological and morphofunctional parameters of barley seeds (*Hordéum vulgáre* L.). *Scientifc Reports* 2023; **13(1)**, 6453.

[37] W Li, Y Wang, J Li, X Guo, Q Song and J Xu. Selenite improves growth by modulating phytohormone pathways and reprogramming primary and secondary metabolism in tomato plants. *Plant Physiology and Biochemistry* 2024; **214**, 108930.

[38] A Ullah, X Yin, F Wang, B Xu, ZA Mirani, B Xu, MWH Chan, A Ali, M Usman, N Ali and M Naveed. Biosynthesis of selenium nanoparticles (via *Bacillus subtilis* BSN313), and their isolation, characterization, and bioactivities. *Molecules* 2021; **26(18)**, 5559.

[40] SM Joshi, SD Britto, S Jogaiah and SI Ito. Mycogenic selenium nanoparticles as potential new generation broad spectrum antifungal molecules. *Biomolecules* 2019; **9(9)**, 419.

[41] OEA Al-Hagar, D Abol-Fotouh, ES Abdelkhalek, MMA Elsoud and NM Sidkey. *Bacillus niabensis* OAB2: Outstanding bio-factory of selenium nanoparticles. *Materials Chemistry and Physics* 2021; **273**, 125147.

[42] FG Martínez, G Moreno-Martin, M Pescuma, Y Madrid-Albarrán and F Mozzi. Biotransformation of selenium by lactic acid bacteria: Formation of seleno-nanoparticles and seleno-amino acids. *Frontiers in Bioengineering and Biotechnology* 2020; **8**, 506.

[43] D Wang, X Xia, S Wu, S Zheng and G Wang. The essentialness of glutathione reductase GorA for biosynthesis of Se (0)-nanoparticles and GSH for

CdSe quantum dot formation in *Pseudomonas stutzeri* TS44. *Journal of Hazardous Materials* 2019; **366**, 301-310.

[44] M Ashengroph and SR Hosseini. A newly isolated *Bacillus amyloliquefaciens* SRB04 for the synthesis of selenium nanoparticles with potential antibacterial properties. *International Microbiology* 2021; **24(1)**, 103-114.

[45] Z Wang, N Li, X Zhou, S Wei, Y Zhu, M Li, J Gong, Y He, X Dong, C Gao and S Cheng. Optimization of fermentation parameters to improve the biosynthesis of selenium nanoparticles by *Bacillus licheniformis* F1 and its comprehensive application. *BMC Microbiology* 2024; **24(1)**, 271.

[46] E Sans-Serramitjana, C Gallardo-Benavente, F Melo, JM Pérez-Donoso, C Rumpel, PJ Barra, P Durán and MDLL Mora. A comparative study of the synthesis and characterization of biogenic selenium nanoparticles by 2 contrasting endophytic selenobacteria. *Microorganisms* 2023; **11(6)**, 1600.

[47] B Hosnedlova, M Kepinska, S Skalickova, C Fernandez, B Ruttkay-Nedecky, Q Peng, M Baron, M Melcova,R Opatrilova, J Zidkova, G Bjørklund, J Sochor and R Kizek. Nano-selenium and its nanomedicine applications: A critical review. *International Journal of Nanomedicine* 2018; **13**, 2107-2128.

[48] DA Al-Quwaie. The influence of bacterial selenium nanoparticles biosynthesized by *Bacillus subtilus* DA20 on blood constituents, growth performance, carcass traits, and gut microbiota of broiler chickens. *Poultry Science* 2023; **102(9)**, 102848.

[49] NT Quach, THN Vu, TTA Nguyen, H Ha, PH Ho, S Chu-Ky, L Nguyen, HV Nguyen, TTT Thanh, NA Nguyen, HH Chu and QT Phi. Structural and genetic insights into a poly-γ-glutamic acid with *in vitro* antioxidant activity of *Bacillus velezensis* VCN56. *World Journal of Microbiology and Biotechnology* 2022; **38(10)**, 173.

[50] MAR Siddique, MA Khan, SAI Bokhari, M Ismail, K Ahmad, HA Haseeb, MM Kayani, S Khan, N Zahid and SB Khan. Ascorbic acid-mediated selenium nanoparticles as potential antihyperuricemic, antioxidant, anticoagulant, and thrombolytic agents. *Green Processing and Synthesis* 2024; **13(1)**, 20230158.

[51] N Shahabadi, S Zendehcheshm and F Khademi. Selenium nanoparticles: Synthesis, *in-vitro* cytotoxicity, antioxidant activity and interaction studies with ct-DNA and HSA, HHb and Cyt c serum proteins. *Biotechnology Reports* 2021; **30**, e00615.

[52] M Safaei, HR Mozaffari, H Moradpoor, MM Imani, R Sharifi and A Golshah. Optimization of green synthesis of selenium nanoparticles and evaluation of their antifungal activity against oral *Candida albicans* infection. *Advances in Materials Science and Engineering* 2022; **2022(1)**, 1376998.

[53] AA Kamnev, PV Mamchenkova, YA Dyatlova and AV Tugarova. FTIR spectroscopic studies of selenite reduction by cells of the rhizobacterium *Azospirillum brasilense* Sp7 and the formation of selenium nanoparticles. *Journal of Molecular Structure* 2017; **1140**, 106-112.

[54] F Wang, M Du, L Kai, S Du, W Hu, Y Wang and Y Cheng. Exopolymer-functionalized nanoselenium from *Bacillus subtilis* SR41: Characterization, monosaccharide analysis and free radical scavenging ability. *Polymers* 2022; **14(17)**, 3523.

[55] GH Ho, TI Ho, KH Hsieh, YC Su, PY Lin, J Yang, KH Yang and SC Yang. γ -Polyglutamic acid produced by *Bacillus subtilis* (natto): Structural characteristics, chemical properties and biological functionalities. *Journal of the Chinese Chemical Society* 2006; **53(6)**, 1363-1384.

[56] P Srithi, N Jarussophon, M Srithaworn and O Chunhachart. *In situ* modification of bacterial cellulose by γ-polyglutamic acid: A comprehensive characterization. *Journal of Food Health and Bioenvironmental Science* 2024; **17(2)**, 56-63.

[57] G Arunşah, A Gűl and EE Hameş-Tuna. Evaluation of a novel antibacterial wound dressing based on bacterial cellulose containing ɣ-PGA/chitosan complex. *In*: Proceedings of the HEZARFEN International Congress of Science, Mathematics and Engineering, Izmir, Turkey. 2019, p. 114-125.

[58] C Dou, Zheng Li, J Gong, Q Li, C Qiao and J Zhang. Bio-based poly (γ-glutamic acid) hydrogels reinforced with bacterial cellulose nanofibers exhibiting superior mechanical properties and cytocompatibility. *International Journal of Biological Macromolecules* 2021; **170(15)**, 354-365.

[59] MT El-Saadony, AM Saad, AA Najjar, SO Alzahrani, FM Alkhatib, ME Shafi, E Selem, ESM Desoky, SEE Fouda, AM El-Tahan and MAA Hassan. The use of biological selenium nanoparticles to suppress *Triticum aestivum* L. crown and root rot diseases induced by *Fusarium* species and improve yield under drought and heat stress. *Saudi Journal of Biological Sciences* 2021; **28(8)**, 4461-4471.

[60] B Nowruzi, BS Jalil and JS Metcalf. Antifungal screening of selenium nanoparticles biosynthesized by microcystin-producing *Desmonostoc alborizicum*. *BMC Biotechnology* 2023; **23(1)**, 41.

[61] AI Perfileva and KV Krutovsky. *Nanotechnology in plant health*. CRC Press, Boca Raton, 2024.

[62] DA Serov, VV Khabatova, V Vodeneev, R Li and SV Gudkov. A review of the antibacterial, fungicidal and antiviral properties of selenium nanoparticles. *Materials* 2023; **16(15)**, 5363.

[63] M Shahbaz, A Akram, NI Raja, T Mukhtar, A Mehak, N Fatima, M Ajmal, K Ali, N Mustafa and F Abasi. Antifungal activity of green synthesized selenium nanoparticles and their effect on physiological, biochemical, and antioxidant defense system of mango under mango malformation disease. *Plos One* 2023; **18(2)**, e0274679.

[64] SH Nile, D Thombre, A Shelar, K Gosavi, J Sangshetti, W Zhang, E Sieniawska, R Patil and G Kai. Antifungal properties of biogenic selenium nanoparticles functionalized with nystatin for the inhibition of *Candida albicans* biofilm formation. *Molecules* 2023; **28**, 1836.